

SparseFormer: Attention-based Depth Completion Network

Frederik Warburg¹
Technical University of Denmark
frwa@dtu.dk

Michael Ramamonjisoa¹
Ecole des Ponts
michael.ramamonjisoa@enpc.fr

Manuel López-Antequera
Meta
mlop@fb.com

Abstract

Most pipelines for Augmented and Virtual Reality estimate the ego-motion of the camera by creating a map of sparse 3D landmarks. In this paper, we tackle the problem of depth completion, that is, densifying this sparse 3D map using RGB images as guidance. This remains a challenging problem due to the low density, non-uniform and outlier-prone 3D landmarks produced by SfM and SLAM pipelines. We introduce a transformer block, SparseFormer, that fuses 3D landmarks with deep visual features to produce dense depth. The SparseFormer has a global receptive field, making the module especially effective for depth completion with low-density and non-uniform landmarks. To address the issue of depth outliers among the 3D landmarks, we introduce a trainable refinement module that filters outliers through attention between the sparse landmarks.

1. Introduction

In depth completion, an image is used to guide the densification of a sparse depth map obtained from a sensor (LiDAR, RealSense, etc.) or 3D landmarks from *e.g.* Structure from Motion (SfM). Depth completion methods can be divided into (1) *very sparse depth completion* that densify depth from SfM landmarks, (2) *sparse depth completion* that densify depth from LiDAR, and (3) *semi-dense depth completion* that densify depth from *e.g.* RealSense/Kinect. The differentiation is important as SfM landmarks are less uniformly distributed, more error prone and much sparser (typically $< 0.1\%$ of pixels have depth) than depth from LiDAR (depth density $\approx 10\%$) or from depth sensors such as RealSense or Kinect (depth density 60 – 90%). Due to the popularity of the KITTI Depth Completion benchmark [19] most depth completion methods have focused on *sparse depth completion* from LiDAR data where depth measurements are spatially uniformly distributed. These methods often fail to produce accurate depth for sparser or less evenly distributed data. In this paper, we present

the SparseFormer, which is specifically designed for *very sparse depth completion* from SfM landmarks.

The core of the SparseFormer is an attention volume between 3D landmarks projected onto the image plane and visual features extracted from a convolutional decoder. This attention volume describes the similarity between each region in an image and each 3D landmark. This can be interpreted as an affinity matrix that can be used to interpolate depth to the entire scene in a single step. The global nature of this affinity allows the model to generalize well to different landmark distributions and sparsity levels. Since the number of SfM landmarks is usually low (≈ 300 per frame), the attention mechanism effectively scales linearly with the feature map resolution, allowing us to compute the attention volume without large memory requirements. To accommodate potential outliers in the input depth, we introduce a refinement module that prevents the SparseFormer from propagating noisy information to the interpolation process. This is achieved by concatenating the depth to the features at those SfM landmarks, and by allowing these depth-aware features to exchange information via a standard transformer.

To validate our approach, we first perform an ablation study on the number of 3D points on an indoor dataset. We find that the SparseFormer especially improves performance even for low densities of points. Then we show on a large outdoor dataset that our approach is effective for *very sparse depth completion* with 3D points obtained from a standard SfM pipeline.

2. Related work

Depth completion has shown superior performance compared to monocular depth prediction and higher versatility and efficiency compared to stereo approaches. Despite impressive performance, depth completion is still a challenging task, where the main challenges stem from fusing different modalities (RGB and depth) and handling sparse data. Existing depth completion methods can be divided into three non-mutually exclusive categories: Early fusion, late fusion, and iterative approaches.

¹ Work was done during internship at Meta.

Early Fusion methods fuse image and depth early in the network. The motivation is that the network can dedicate all of its capacity to optimally combine the modalities through training. Early works on depth completion focused on early fusion and tried to make convolutions handle sparse data better. [19] proposed sparsity invariant convolutions, which normalize the convolutional operator by the number of sparse points in its receptive field. [8] proposed to use normalized convolutions to propagate a binary [8, 9] or continuous learned [7] confidence through the network. These methods strive to make the convolutions handle sparse data better, but do not deal with the computational overhead of convolving regions without any information, which is the case for most regions in *very sparse depth completion*. Other approaches have tried to densify the sparse input depth before feeding it to the network. [2] proposed to achieve this with nearest neighbor upsampling, while also modelling the distance to the closest sparse point. [22] used scaffolding to densify the sparse input depth. For *sparse and semi-dense depth completion*, where the input depth is rather uniformly distributed, good performance can also be achieved by simple concatenation of image and depth [15, 11, 21]. ACDCNet [21] obtains impressive results by using a channel exchanging network, which allows the network exchange information between different modalities throughout the network, fusing depth from SfM landmarks, depth from a RealSense sensor and an image.

The downside of early fusion methods is that they do not preserve depth and that they do not perform well when the sparse data is not uniformly distributed or too sparse, which is the focus of this paper. Our main insight is that transformers are more suited for very sparse data than convolutions.

Late Fusion methods explicitly guide the depth completion process by first extracting features from the image and using these features to guide a depth interpolation process. GuideNet [18] proposed to imitate guided filtering by learning a spatial variant kernel, ENet [11] simplified this by an element-wise multiplication of features from input depth and features from an image. RigNet [24] proposes a repetitive image guided network with an adaptive guidance of depth. These late fusion approaches have state-of-the-art performance on the KITTI depth completion benchmark [19]. We follow this strategy and insert our proposed SparseFormer module in the decoder.

Iterative Fusion methods merge sparse depth and a predicted depth map in depth space. A network predicts initial depth and affinities and the initial depth is updated iteratively using the learned affinities. This merging constrains the network to preserve depth when it is available, while having smoothness between predicted depth and sparse depth. SPN [13] was the first to propose to predict affinities followed by an iterative diffusion. CSPN [4] pro-

posed to predict affinities to the 8 nearest neighbors in a grid, and showed that the iterative updates can efficiently be computed with convolutions. CSPN++ [3] proposed a more efficient diffusion process by using kernels with different strides and predicting the number of iterative update steps. PeNET [11] proposes to accelerate CSPN++ by better parallelization. NLSPN [16] uses deformable convolutions to avoid the grid constraint of previous works. GDC [25] does not predict affinities, but estimates them in 3D based on local similarity and updates depth in 3D by optimizing a constraint graph. [23] also models the diffusion in 3D, but uses a graph-convolutional network to update depth of point neighborhoods. The downside of these approaches is the iterative update, which is slow, and therefore often constrained to 10 – 30 update steps. The affinities model depth similarity between neighboring points (in 2D or 3D), not allowing information to diffuse globally, *e.g.* observing a sparse point on a plane fronto-parallel to the camera sensor should describe the depth of the entire plane, however, these methods cannot diffuse depth to distant regions as the number of update steps has to be kept rather small for computational reasons. In contrast, the SparseFormer is a global approach that enables the diffusion of depth to the entire scene in one update.

Transformers: Recent work has shown that transformers outperform convolutional approaches across many tasks such classification [6], object detection [1] and depth prediction [17]. The core of transformers is the attention mechanism that gives the networks a global receptive field. Standard attention scales quadratically with the image size. Multiple recent works have tried to come up with general solutions that can alleviate the huge memory requirement for naive attention. [6] proposed to divide the image into patches and perform attention between the patches. Other approaches [20, 12, 5] propose to approximate the attention volume. The nature of the problem of very sparse depth completion allows us to sidestep the issue: Since the number of sparse features with depth, in our setting, is very low, our attention module effectively scales linearly rather than quadratically with the image size.

3. Method

The proposed method consists of T SparseFormers that can be inserted in any decoder to enrich the features with global depth information. Each SparseFormer can be viewed as a learned, global diffusion process. Fig. 1 serves as an overview of our method. The SparseFormer takes deep features and 3D landmarks projected into the image plane as input and outputs a dense depth and confidence map, which are used to enrich the convolutional features.

SparseFormer. The goal of each SparseFormer is to diffuse depth and confidence from a few 3D points to enrich

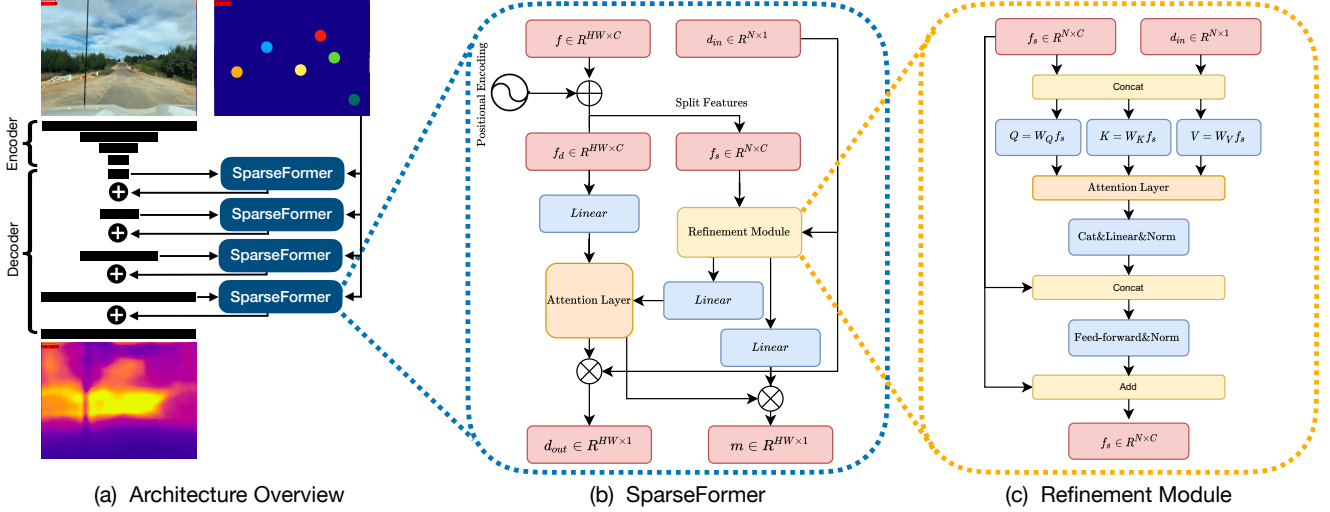


Figure 1: **(a) Architecture overview.** We insert 4 SparseFormers into a depth prediction encoder-decoder architecture [10]. **(b) SparseFormer.** The SparseFormer takes a convolutional feature map f , and N 3D sparse points as input and outputs an interpolated depth map d_{out} and a confidence map m . **(c) Refinement module.** The refinement module fuses deep features of SfM points and their associated depth, allowing the features to communicate via attention.

deep convolutional features. *E.g.* if a sparse point is observed on a plane, we aim to diffuse the known depth to the entire plane. In contrast to iterative methods [13, 4, 3, 16], the SparseFormer can learn to diffuse information to the entire scene - making the module highly flexible and adaptive to different point densities and distributions.

The SparseFormer takes deep features $f \in R^{H \times W \times C}$ from a traditional convolutional decoder and N 3D points as input, and outputs a dense depth map $d_{out} \in R^{H \times W}$ and a confidence map $m \in R^{H \times W}$. The SparseFormer is specifically designed for situations where $N \ll HW$ and where the N points can contain outliers. This is in contrast to previous works [25, 16, 4] that assume that the provided sparse depth is always reliable.

Fig. 1 (b) gives an overview of a SparseFormer. A positional encoding is concatenated with the dense input features, which are then flattened $f_d \in R^{HW \times C}$. From these features, sparse features $f_s \in R^{N \times C}$ are extracted for each 3D point. The sparse features are refined in order to remove outliers (explained in Sec. 3 and Fig. 1 (c)). We then learn an attention volume $A \in R^{HW \times N}$ that describes the similarity between each feature and the N 3D points.

$$A = \text{Softmax} \left(\frac{(W_q f_s)(W_k f_d)^T}{\sqrt{C}} \right) \quad (1)$$

where W_q, W_k are learnable weights. Since N is small (< 500), this attention volume scales approximately linearly with the feature resolution, thus can be computed in high resolution with a relatively low memory footprint.

The attention volume can be interpreted as learned interpolation weights based on feature similarity and posi-

tional similarity. We use A to interpolate dense depth $d_{out} \in R^{HW \times 1}$ and confidence $m \in R^{HW \times 1}$

$$d_{out} = A d_{in} \quad (2)$$

$$m = W_o(A(W_v f_s)) \quad (3)$$

where W_o, W_v are learnable weights.

The interpolated depth d_{out} and confidence m is merged with the features from the convolutional decoder with a 1×1 convolutional layer.

Refinement Module. The refinement module has three objectives: (1) add depth information to the deep features, and allow the features to communicate to (2) filter outliers and (3) improve the depth. Fig. 1 (c) gives an overview of the refinement module. First, deep features for each of the 3D points are concatenated with their associated depth to add depth information. Then, these concatenated features are fed through a standard transformer with self-attention. The transformer improves the feature of each 3D point by allowing it to share information between the other landmarks. The transformer can also filter 3D points with erroneous depth, which are common in SfM pipelines due to *e.g.* wrong 2d-2d matches. It can achieve this by learning a mapping that sends these features far away from the rest of the features in the embedding space. This is important in order to not propagate erroneous depth to the interpolation stage.

Handling varying levels of depth sparsity. The number of sparse depth points vary from scene to scene. In order

Architecture	Authors	#3D points	REL	RMSE	a1	a2	a3
NLSPN [16]	Park'20	2	0.300	1.152	0.393	0.697	0.879
SparseFormer		2	0.161	0.626	0.740	0.937	0.984
NLSPN [16]	Park'20	32	0.114	0.554	0.825	0.947	0.985
SparseFormer		32	0.050	0.255	0.962	0.992	0.998
NLSPN [16]	Park'20	200	0.019	0.136	0.989	0.998	0.999
SparseFormer		200	0.022	0.142	0.989	0.998	1.000
NLSPN [16]	Park'20	500	0.012	0.092	0.996	0.999	1.000
SparseFormer		500	0.014	0.104	0.994	0.999	1.000

Table 1: **Results on NYUDv2.** The SparseFormer outperforms NLSPN when few points are available. This is due to the global receptive field of the SparseFormer that diffuses depth to all regions in the image. Both methods use a Resnet34 encoder.

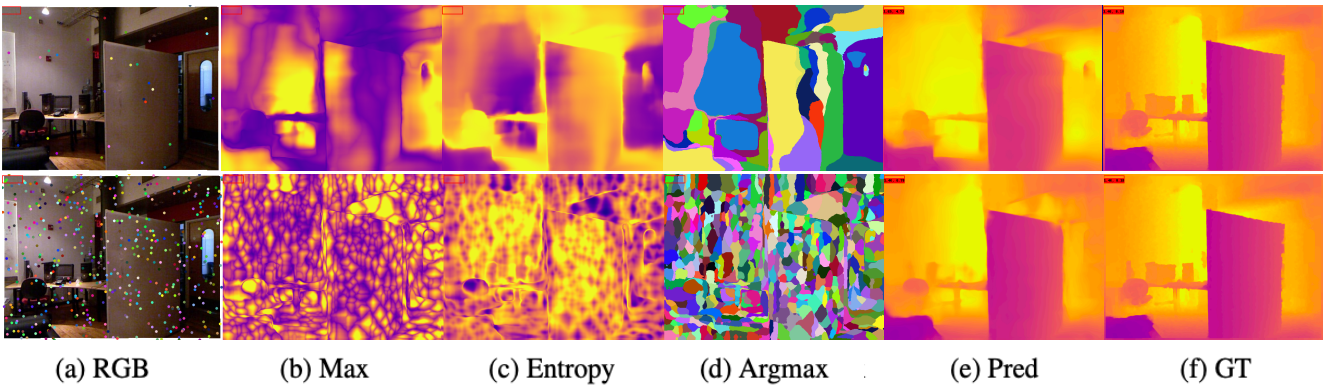


Figure 2: **Visualization of global depth diffusion.** *From left to right:* RGB image with sparsely sampled ground-truth points emulating 3D landmarks, maximum over attention values, entropy over attention volume, argmax over attention volume color-coded to match to the sparse point in the RGB image for respectively 32 and 500 sampled points. The SparseFormer adapts to very different input depth densities. The points are interpolated in a local area thanks to the positional encoding. The interpolation clearly respects boundaries at depth discontinuities. Notice how the interpolation is vertical on walls whereas on fronto-parallel surfaces the interpolation is omni-directional.

to handle the varying number of point densities and to train in an efficiently batched way, the number of 3D points is fixed. This is done by padding, if the scene contains fewer points than the specified threshold and through random selection if the scene contains more sparse depth points than the specified threshold.

4. Experimental Results

We insert 4 SparseFormers in the decoder of the Monodepth2 [10]. We supervise the final output prediction as well as the interpolated depth map of each SparseFormer, such that our final loss becomes $\sum_s w_s (l_1 + l_2)$ where s iterates over scales and $w_s = (1.0, 0.5, 0.25, 0.15, 0.10)$. We use an Adam optimizer ($\beta_1 = 0.9, \beta_2 = 0.999$) and train for 600k iterations with learning rate 0.001, which is decayed by 80% every 200k iterations. We use batch size 24.

We train and evaluate our model on two datasets: The

NYU Depth dataset and the Mapillary Planet-Scale Depth dataset. For quantitative comparison, we report the following commonly used metrics [16].

$$\text{REL: } \frac{1}{|\mathcal{V}|} \sum_{v \in \mathcal{V}} |(d_v^{gt} - d_v^{pred}) / d_v^{gt}| \quad (4)$$

$$\text{RSME: } \sqrt{\frac{1}{|\mathcal{V}|} \sum_{v \in \mathcal{V}} |d_v^{gt} - d_v^{pred}|^2} \quad (5)$$

$$\delta_t : \max \left(\frac{d_v^{gt}}{d_v^{pred}}, \frac{d_v^{pred}}{d_v^{gt}} \right) < \tau \quad (6)$$

NYU Depth V2. (NYUDv2) [19] is an indoor dataset where ground truth is obtained with a Kinect sensor.

We follow a similar procedure to [16] and use a subset of $\approx 50k$ images from the official training split and the offi-

Architecture	REL	RMSE	a1	a2	a3
Monodepth2 [10]	0.052	15.777	0.895	0.943	0.970
ENet [11]	0.019	5.469	0.975	0.988	0.992
SparseFormer	0.011	4.948	0.989	0.996	0.998

Table 2: **Results on MPSD.** All methods use a Resnet101 encoder.

cial test split of 654 images for evaluation and comparisons. Each image was downsized to a resolution of 320×240 , and then center-cropped to 304×228 pixels.

Fig. 2 illustrates the diffusion mechanism for a varying number of available sparse points. Note how the attention mechanism adapts to the number of sparse points. The depth is diffused to large neighborhoods when only few points are available.

Tab. 1 shows that our model outperforms NLSPN when very few 3D points are available, and matches the predictive performances of NLSPN when more points are available.

MPSD We first compute SfM landmarks on the Mapillary Planet-Scale Depth (MPSD) [14] dataset. The dataset contains ≈ 1 M images with a large geographical coverage. The SfM landmarks are generated with OpenSfM using SIFT features, thus representing a typical scenario for *very sparse depth completion*.

Fig. 3 shows that neither the ground-truth depth nor the input 3D points are uniformly distributed in the image, but rather clustered in textured areas and around boundaries. The average density of the 3D points is 0.1% (330 points per frame), whereas the density of the ground-truth is 16% (50k points per frame).

Fig. 4 shows the distribution of the SfM depth and the ground-truth depth. The SfM points are on average further away from the camera than the ground-truth depth on this dataset.

We compare against two recent methods, which use a Resnet101 as backbone. (1) Monodepth2 [10] which we train supervisedly, and adapt to depth completion by concatenating the RGB and sparse depth inputs. (2) ENet [11], which is one of the top performing methods on the KITTI depth completion dataset. Tab. 2 shows that the SparseFormer outperforms both baselines due to its global receptive field and the communication between the sparse features.

Fig. 5 shows qualitative results from the SparseFormer. The SparseFormer produces accurate depth maps using a few sparse SfM landmarks and RGB images.

5. Conclusion

We propose a transformer module for *very sparse depth completion*. The SparseFormer is specifically designed for

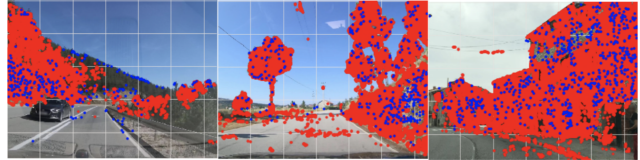


Figure 3: SfM landmarks projected into the camera (blue) and the ground-truth depth (red).

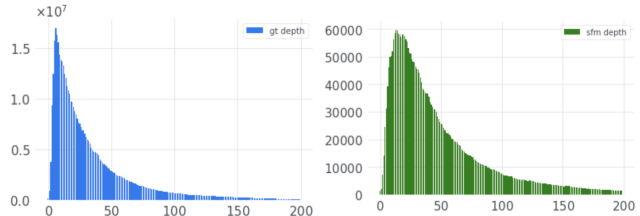


Figure 4: Depth distribution of SfM landmarks and ground-truth in meters. SfM landmarks are on average further away than the ground-truth depth.

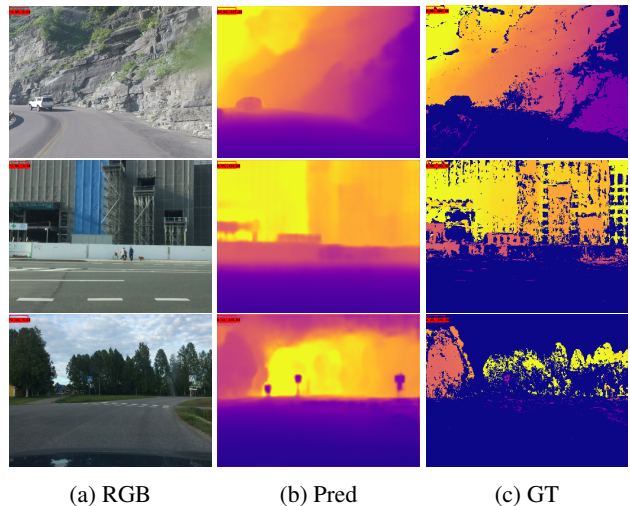


Figure 5: **Qualitative results on MPSD.** The SparseFormer learns to produce accurate depth maps using an image and 3D points as input and semi-dense depth as supervision.

low density, non-uniformly distributed and outlier prone 3D depth. The SparseFormer consists of (i) an interpolation module that globally interpolates 3D points based on visual similarity and position, which allow the network to globally diffuse depth. (ii) A refinement module that fuses depth and visual features and filters outliers through cross-attention of the sparse points. We demonstrate on both indoor and outdoor datasets that the proposed SparseFormer is effective in low density depth completion.

References

- [1] Nicolas Carion, Francisco Massa, Gabriel Synnaeve, Nicolas Usunier, Alexander Kirillov, and Sergey Zagoruyko. End-to-end object detection with transformers. *Eur. Conf. Comput. Vis.*, 2020. 2
- [2] Zhao Chen, Vijay Badrinarayanan, Gilad Drozdov, and Andrew Rabinovich. Estimating depth from RGB and sparse sensing. *Eur. Conf. Comput. Vis.*, 2018. 2
- [3] Xinjing Cheng, Peng Wang, Chenye Guan, and Ruigang Yang. CSPN++: learning context and resource aware convolutional spatial propagation networks for depth completion. *AAAI*, 2019. 2, 3
- [4] Xinjing Cheng, Peng Wang, and Ruigang Yang. Learning depth with convolutional spatial propagation network. *Eur. Conf. Comput. Vis.*, 2018. 2, 3
- [5] Krzysztof Choromanski, Valerii Likhoshesterov, David Dohan, Xingyou Song, Andreea Gane, Tamás Szepesvári, Peter Hawkins, Jared Davis, Afroz Mohiuddin, Lukasz Kaiser, David Belanger, Lucy J. Colwell, and Adrian Weller. Rethinking attention with performers. *Int. Conf. Learn. Represent.*, 2020. 2
- [6] Alexey Dosovitskiy, Lucas Beyer, Alexander Kolesnikov, Dirk Weissenborn, Xiaohua Zhai, Thomas Unterthiner, Mostafa Dehghani, Matthias Minderer, Georg Heigold, Sylvain Gelly, Jakob Uszkoreit, and Neil Houlsby. An image is worth 16x16 words: Transformers for image recognition at scale. *Int. Conf. Learn. Represent.*, 2020. 2
- [7] Abdelrahman Eldesokey, Michael Felsberg, Karl Holmquist, and Mikael Persson. Uncertainty-aware cnns for depth completion: Uncertainty from beginning to end. *IEEE Conf. Comput. Vis. Pattern Recog.*, 2020. 2
- [8] Abdelrahman Eldesokey, Michael Felsberg, and Fahad Shahbaz Khan. Confidence propagation through cnns for guided sparse depth regression. *IEEE Trans. Pattern Anal. Mach. Intell.*, 2018. 2
- [9] Abdelrahman Eldesokey, Michael Felsberg, and Fahad Shahbaz Khan. Propagating confidences through cnns for sparse data regression. *Brit. Mach. Vis. Conf.*, 2018. 2
- [10] Clément Godard, Oisín Mac Aodha, Michael Firman, and Gabriel J. Brostow. Digging into self-supervised monocular depth prediction. *Int. Conf. Comput. Vis.*, 2019. 3, 4, 5
- [11] Mu Hu, Shuling Wang, Bin Li, Shiyu Ning, Li Fan, and Xiaojin Gong. Penet: Towards precise and efficient image guided depth completion. *IEEE Int. Conf. Robotics and Automation.*, 2021. 2, 5
- [12] Nikita Kitaev, Lukasz Kaiser, and Anselm Levskaya. Reformer: The efficient transformer, 2020. 2
- [13] Sifei Liu, Shalini De Mello, Jinwei Gu, Guangyu Zhong, Ming-Hsuan Yang, and Jan Kautz. Learning affinity via spatial propagation networks. *Adv. Neural Inform. Process. Syst.*, 2017. 2, 3
- [14] Manuel Lopez-Antequera, Pau Gargallo, Markus Hofinger, Samuel Rota Buló, Yubin Kuang, and Peter Kotschieder. Mapillary planet-scale depth dataset. 2020. 5
- [15] Fangchang Ma and Sertac Karaman. Sparse-to-dense: Depth prediction from sparse depth samples and a single image. *IEEE Int. Conf. Robotics and Automation.*, 2018. 2
- [16] Jinsun Park, Kyungdon Joo, Zhe Hu, Chi-Kuei Liu, and In So Kweon. Non-local spatial propagation network for depth completion. *Eur. Conf. Comput. Vis.*, 2020. 2, 3, 4
- [17] René Ranftl, Alexey Bochkovskiy, and Vladlen Koltun. Vision transformers for dense prediction. *Int. Conf. Comput. Vis.*, 2021. 2
- [18] Jie Tang, Fei-Peng Tian, Wei Feng, Jian Li, and Ping Tan. Learning guided convolutional network for depth completion. *IEEE Trans. Image Process.*, 2021. 2
- [19] Jonas Uhrig, Nick Schneider, Lukas Schneider, Uwe Franke, Thomas Brox, and Andreas Geiger. Sparsity invariant cnns. In *3DV*, 2017. 1, 2, 4
- [20] Sinong Wang, Belinda Z. Li, Madian Khabsa, Han Fang, and Hao Ma. Linformer: Self-attention with linear complexity. *Adv. Neural Inform. Process. Syst.*, 2020. 2
- [21] Frederik Warburg, Daniel Hernandez-Juarez, Juan Tarrio, Alexander Vakhitov, Ujwal Bonde, and Pablo F. Alcantarilla. Self-supervised depth completion for active stereo, 2021. 2
- [22] Alex Wong, Xiaohan Fei, and Stefano Soatto. VOICED: depth completion from inertial odometry and vision. *IEEE Int. Conf. Robotics and Automation.*, 2019. 2
- [23] Xin Xiong, Haipeng Xiong, Ke Xian, Chen Zhao, Zhiguo Cao, and Xin Li. Sparse-to-dense depth completion revisited: Sampling strategy and graph construction. In *ECCV*, 2020. 2
- [24] Zhiqiang Yan, Kun Wang, Xiang Li, Zhenyu Zhang, Baobei Xu, Jun Li, and Jian Yang. Rignet: Repetitive image guided network for depth completion. *CoRR*, abs/2107.13802, 2021. 2
- [25] Yurong You, Yan Wang, Wei-Lun Chao, Divyansh Garg, Geoff Pleiss, Bharath Hariharan, Mark Campbell, and Kilian Q. Weinberger. Pseudo-lidar++: Accurate depth for 3d object detection in autonomous driving. *Int. Conf. Learn. Represent.*, 2019. 2, 3